Ultrasonics 133 (2023) 107056

Contents lists available at ScienceDirect

Ultrasonics

journal homepage: www.elsevier.com/locate/ultras

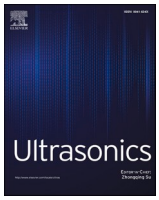

Dual-drug loaded ultrasound-responsive nanodroplets for on-demand combination chemotherapy

Catalina-Paula Spatarelu [a], Sidhartha Jandhyala [a], Geoffrey P. Luke [a,b,*]

[a] Thayer School of Engineering, Dartmouth College, 15 Thayer Drive, Hanover, NH 03755, United States
[b] Translational Engineering in Cancer Research Program, Dartmouth Cancer Center, 1 Medical Center Drive, Lebanon, NH 03766, United States

ARTICLE INFO

Keywords:
Combination chemotherapy
Ultrasound-sensitive
Perfluorocarbon

ABSTRACT

Phase-changing nanodroplets are nanometric sized constructs that can be vaporized via external stimuli, such as focused ultrasound, to generate gaseous bubbles that are visible in ultrasound. Their activation can also be leveraged to release their payload, creating a method for ultrasound-modulated localized drug delivery. Here, we develop a perfluoropentane core nanodroplet that can simultaneously load paclitaxel and doxorubicin, and release them in response to an acoustic trigger. A double emulsion method is used to incorporate the two drugs with different physio-chemical properties, which allows for a combinatorial chemotherapy regimen to be used. Their loading, release, and biological effects on a triple negative breast cancer mouse model are investigated. We show that activation enhances the drug-delivery effect and delays the tumor growth rate in vivo. Overall, the phase-changing nanodroplets are a useful platform to allow on-demand delivery of combinations of drugs.

1. Introduction

One of the hallmarks of cancer that make tumors challenging to treat is acquired resistance to treatments that can occur early on in the regimen [1]. To address this challenge, the use of multiple therapeutic treatments, often called "combination therapy," has been tested and adopted in several types of cancer [2,3]. Combination chemotherapy often allows oncologists to reduce the dosage of each drug and achieve better efficacy than single-agent therapy. In spite of its widespread use, combination therapy still comes with limitations. Agents have to be chosen in such a manner that they target different disease pathways and that their effects towards cancer cells are neutral or synergistic. The administration of multiple drugs is not straightforward, as their different properties are bound to result in dissimilar pharmacokinetic and biodistribution profiles. Furthermore, optimized dosage is dependent on a multitude of factors such as drug interactions, presence of certain tumor biomarkers, potential side effects and others [2,4].

Nanomedicine has emerged as an appealing strategy to control the ratios and pharmacokinetic profiles of multiple drugs *in vivo* [3]. By unifying the pharmacokinetics of the two or more drugs at a particular predetermined loading ratio, the degree of synergism can be tuned to achieve improved therapeutic effects [5]. The clinical adoption of nanomedicine, however, has been slowed by its passive drug release and overreliance on the enhanced permeation and retention (EPR) effect, which is heavily impaired by intra-, and inter- tumor heterogeneity [6,7].

Perfluorocarbon (PFC) nanodroplets are a multifunctional technology that have the potential to improve nanotherapeutics via activated release of cargo. They have been proposed for use in preclinical models of cancer, atherosclerosis, and tissue ablation [8–10]. These particles consist of a PFC core stabilized by a surfactant, polymer, or lipid layer, and dispersed in an aqueous media. benefiting from being biocompatible even at large doses, with no significant toxicity or carcinogenicity, and a half-life on the order of hours in vivo [11]. When exposed to the proper stimulus – acoustic energy, optical energy, or magnetic energy – nanodroplets can be noninvasively disrupted, releasing their cargo [12–14]. Nanodroplets loaded with doxorubicin [15] and paclitaxel [16,17] have resulted in effective tumor responses when combined with ultrasound activation. This demonstrates the benefit of the precise spatiotemporal control of drug delivery that PFC nanodroplets provide.

In addition to releasing the encapsulated cargo, the vaporization event can result in additional biomechanical effects. Activation of PFC nanodroplets has been shown to temporarily or irreversibly permeate nearby cellular membranes in a process known as sonoporation [18].

Abbreviations: EPR, enhanced permeation and retention; PFC, perfluorocarbon; ADV, acoustic droplet vaporization; DDD, dual-drug loaded nanodroplet.

* Corresponding author at: Thayer School of Engineering, Dartmouth College, 15 Thayer Drive, Hanover, NH 03755, United States.
E-mail address: geoffrey.p.luke@dartmouth.edu (G.P. Luke).

https://doi.org/10.1016/j.ultras.2023.107056
Received 12 January 2023; Received in revised form 13 May 2023; Accepted 23 May 2023
Available online 26 May 2023
0041-624X/

This has been applied to disrupt the endothelial barrier, enabling the delivery of macromolecules into the interstitial space [19–21]. In the case of acoustic droplet vaporization (ADV), two mechanisms are thought to be responsible for cell sonoporation: 1) the rapid phase transition from liquid to gas and bubble evolution and 2) the behavior of the resulting bubbles under continued ultrasound exposure (i.e., cavitation and displacement)[18]. Factors such as the distance between bubbles and cells, nanodroplet concentration, and ultrasound intensity were investigated *in vitro* [22–24], showing good promise for the application of such constructs in vivo.

In this work, we aimed to investigate the effects of activation upon the cytotoxicity of a combination therapy regimen, co-encapsulated in phase-changing nanodroplets. We developed a dual-drug loaded nanodroplet (DDD) platform with the ability to load versatile combinations of hydrophobic and hydrophilic drugs. Here, we used doxorubicin and paclitaxel, drugs that are commonly used together in the clinic due to their different mechanisms of action and ratio-dependent synergistic effects [5,25,26]. The DDDs can be externally activated with pulsed focused ultrasound and release the loaded therapeutics. Loading both these drugs in nanodroplets bypasses the issue of different pharmacokinetic profiles [27], ensuring the co-delivery at the same time and place. The biological effects of acoustical activation of the DDDs are investigated in vitro and in a triple negative breast cancer xenograft mouse model. The results show that the active drug release is more effective than simply relying on passive DDD accumulation through the EPR effect.

2. Materials and methods

2.1. Synthesis of nanodroplets

The DDDs were synthesized by a double emulsion method. The first emulsion was synthesized by a thin-layer hydration-sonication method. A mixture of dipalmitoylphosphatidylcholine (DPPC, NOF America), 1,2-distearoyl-*sn*-glycero-3-phosphoethanolamine-N-[amino(polyethylene glycol)-2000] (DSPE-$PEG_{2000,}$ NOF America) and cholesterol (Alfa Aesar), in a molar ratio of 35:15:50 was added to 3 mL chloroform (Alfa Aesar) and evaporated under vacuum (250 mbar) with a rotary evaporator at 38.5 °C and 30 rpm. The solution contained 5 mmol total lipid mixture. Paclitaxel (2 mg, Fisher Scientific) was dissolved together with the lipids in chloroform for co-assembly. After the mixture evaporated and formed a thin film, 3 mL of 2:3 v/v water: Dulbecco's phosphate-buffered saline (Corning) was used for rehydration, and the mixture was subjected to a 35-kHz sonicating bath (VWR Symphony) for 5 min at room temperature. Next, the mixture was dispersed with a sonication probe (QSonica, Q700, 1/8-inch microtip) for 30 s continuously, at 27 W/cm^2 in an ice-bath to prevent the sample from overheating.

The second emulsion was constituted by aqueous doxorubicin solution (Advanced ChemBlocks) in perfluoropentane (PFP, Fluoromed). The doxorubicin solution (0.25 mL, 7.0 mg/mL) was added to a mixture of PFP (1.5 mL) and emulsifier (Krytox™ FSL, Chemours, 20 μL) and sonicated with the ultrasonic probe under the same conditions described before. A volume of 200 μL of this emulsion was added to the lipid-paclitaxel mixture and sonicated for an additional 30 s on the same settings as above. For empty nanodroplets, this step consisted of only adding the PFP, followed by the same sonication regimen.

The nanodroplet mixture was centrifuged with an Eppendorf MiniSpin centrifuge at 43 rcf for 60 s to remove large aggregates and unencapsulated components, such as paclitaxel, that settle out of the dispersion due to poor solubility in water. This was followed by collecting of the supernatant and two more steps of centrifugation at 2100 rcf for 60 s each. For each of these steps, the supernatant was discarded and replaced with 3 mL distilled water to remove micelles and unincorporated doxorubicin.

To obtain fluorescent nanodroplets that can be visualized with near-infrared (NIR) fluorescence, 40 μL of a 1 mg/mL 1,1′-dioctadecyl-3,3,3′,3′-tetramethylindotricarbocyanine iodide (DiR, Biotium) dye solution in chloroform was added together with the lipids in the synthesis of the nanodroplets. The doxorubicin in the core was omitted, as was the paclitaxel in the shell. All the rest of the synthesis and washing steps were the same as for the DDDs.

2.2. Size and charge characterization

Average nanodroplet diameter and size distribution were determined by a Malvern Zetasizer Dynamic Light Scattering (DLS) instrument after 100x dilution to ensure the concentration was low enough for single-scattering events. All samples were subjected to 3 measurements each, with no delay between measurements, with an automatic number of runs per measurement, as determined by the instrument. Size is reported as the intensity-weighted size distribution.

For zeta potential determination, nanodroplets were diluted in a 0.01 M NaCl (LabChem) solution and measured with a Malvern Nano Zetasizer for 3 measurements with an automatically determined number of runs/measurement. The zeta potential is shown as an intensity-weighted distribution.

2.3. Drug loading measurement

The nanodroplets were dissolved in a 50/50 v/v mixture of acetonitrile (ACN, Alfa Aesar) and water and heated to 60 °C for 30 min to ensure the destruction of all droplets. The paclitaxel concentration was determined by UV–VIS (Varian Cary® 50, Agilent) absorption at 229 nm, by means of a previously constructed calibration curve. For doxorubicin measurements, the nanodroplets were dissolved in a 50/50 v/v mixture of ethanol and water and allowed to dissolve completely. Doxorubicin content was measured by a Horiba FluoroMax spectrofluorometer, using an excitation wavelength of 480 nm and emission at 590 nm, against a previously constructed calibration curve. All doxorubicin-loaded samples were shielded from light between preparation and measurement to avoid quenching.

The encapsulation efficiency, *ee*, was determined by the formula:

$$ee, \% = \frac{amountofdrugmeasured, mg}{amountofdrugaddedinitially, mg} \times 100 \quad (1)$$

2.4. Drug release study

Nanodroplets were dispersed in distilled water in a 24-well plate and subjected to acoustic activation by a single-element ultrasound transducer (Sonic Concepts H-151, 1.1 MHz, 10 pulses of 10 cycles each with a peak focal pressure of 9.6 MPa) powered by a radiofrequency power amplifier (E&I 1020L). The transducer was coupled to the bottom of the plate with polyacrylamide gel focusing cone. The methods for creating the cone are detailed in our previous paper [28]. Ultrasound gel was applied to each interface to facilitate acoustic transmission. The 24-well plate was agitated after each ultrasound pulse to enable activation of a large population of DDDs. The pressure level and number of cycles were selected after applying ultrasound to a sample of DDDs and visually observing bubble generation. The acoustic pressure was previously calibrated using a needle hydrophone (Precision Acoustics) [29]. Briefly, the hydrophone and ultrasound transducer were submerged in a degassed water bath. The hydrophone was raster scanned with a 3-axis linear stage (Thor Labs) to align it with the focal point of the transducer. The voltage of the transducer excitation waveform was gradually ramped up while measuring the resulting peak pressure for calibration. The experimental setup for activation is depicted in Fig. 1.

After activation, the samples were centrifuged at 2100 rcf for 60 s, and both the supernatant and pellet collected. For paclitaxel measurements, both the supernatant and pellet were dissolved in an ACN/water 1:1 mixture and measured with UV–VIS. For the doxorubicin

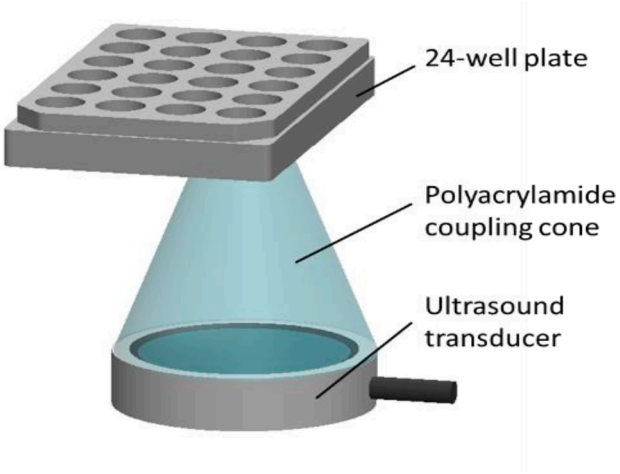

Fig. 1. Experimental setup for activating the nanodroplets for the drug release and cell cytotoxicity studies.

measurements, supernatant and pellet parts were dissolved in 1:1 ethanol/water mixture and measured at 480/590 nm with the fluorospectrometer as described above. For each of the samples, a non-activated control was also measured using the same procedure. The percentage of drug released for each of the drugs was computed by the formula:

$$\%released = \frac{amountofdruginsupernatant, mg}{(amountofdruginsupernatant + amountofdruginpellet), mg} \times 100 \quad (2)$$

2.5. In-vitro cell toxicity studies

MDA-MB-231 cells (ATCC) were used to assess the cytotoxicity of drug-loaded nanodroplets. Cells were passaged and seeded into 24-well plates (Corning) in Dulbecco's Modified Eagle Medium (DMEM, Corning) with 10% fetal bovine serum (FBS, Hyclone), and 1% mixture of penicillin/streptomycin (Corning) at a 0.04 $\times$ 10^6 cells/well density. The cells were left overnight to attach and grow in an incubator at 37 °C and 5% CO_2 concentration, then subjected to various formulations. The studied groups were: non-treated cells for control, inactivated empty nanodroplets, inactivated DDDs, free paclitaxel + doxorubicin, ultrasound-activated empty nanodroplets and ultrasound-activated DDDs. Nanodroplets were added to a 250x dilution in the total volume of each well, or approximately 4.56 $\times$ 10^7 nanodroplets/well. The concentration of loaded paclitaxel was 1.7 μM and that of loaded doxorubicin was 0.28 μM with respect to the well volume in the wells that were subjected to drug-loaded nanodroplets. For the free drug formulation, the same concentrations of both paclitaxel and doxorubicin were used. Each group was triplicated. After adding the corresponding formulation, the cells were allowed to rest for 30 min in the incubator, followed by the subsequent ultrasound activation with the 1.1-MHz transducer (Sonic Concepts H-151) was used at a focal pressure of 9.6 MPa. 10 pulses of 10 cycles. The experimental setup in Fig. 1 was used for ultrasound activation. The cells were then incubated for 4 h, followed by washing with phosphate buffer solution (PBS) and a (3-(4,5-dimethylthiazol-2-yl)-2,5-diphenyltetrazolium bromide) (MTT, Alfa Aesar) assay to assess cell viability. Statistical analysis was performed by using a Student's *t*-test with a Bonferroni correction to account for the multiple experimental groups. A value of $p < 0.05$ was taken to indicate statistically significant differences between the groups.

2.6. Nanodroplets biodistribution and tumor accumulation

To assess the biodistribution of nanodroplets, a Nu/Nu mouse model (Charles River) was used and inoculated with bilateral hind flank tumors by subcutaneous injection. MDA-MB-231 cells (ATCC), a triple negative breast cancer cell line, was employed. The cells were grown in 10% FBS, 1% penicillin/streptomycin enriched DMEM media, until a 90% degree of confluence. They were detached using 0.5% trypsin (Corning) and counted with a hemocytometer (Neubauer chamber, Marienfeld). After centrifuging the cells, the media was replaced with PBS and the cells resuspended by gentle mixing. The cell suspension was then mixed in a 1:1 vol ratio with Matrigel (Corning), and injected in the hind flanks of mice, with each flank receiving approximately 1.5 $\times$ 10^6 cells in a 100-μL volume. Tumors were allowed to grow for three weeks, until they reached a size of approximately 20 mm^3, as measured by ultrasound (Visualsonics Vevo 770, 40 MHz transducer).

The DiR-loaded nanodroplets were employed and NIR fluorescence imaging (Li-Cor Pearl Impulse) was used, imaging the mice prior to activation, immediately after the activation, and for several timepoints afterwards. The mice received a tail vein injection of 100 μL fluorescent nanodroplets dispersion, at a 10x dilution with respect to the stock. The tumor to be activated was assigned randomly, and a 515-kHz annular single-element ultrasound transducer (H-204, Sonic Concepts) was used to activate the tumor, immediately after injection, for a total duration of 10 min, with ultrasound pulses at every 20 s, 10 cycles/pulse and a peak focal pressure of 5.7 MPa. This transducer was used for in-vivo studies because it has a hole in the center of its aperture that allows enables precise alignment of the ultrasound focus with the tumor. The pressure level and number of cycles were selected after applying ultrasound to a sample of DDDs and visually observing bubble generation. All imaging, injection and activation of the tumor were done under anesthesia with isoflurane (VetOne), at a 2% concentration in oxygen, with a flow rate of 1.5 L/h.

At 2 h post-injection, the mice were sacrificed by cervical dislocation while under anesthesia and both tumors were excised and fluorescence images were acquired using the same settings as the whole-body imaging.

2.7. Dual-drug loaded nanodroplets In-vivo efficacy

The same model of triple negative breast cancer as described in the previous section was employed. Each mouse was inoculated with two hind flank tumors by injecting a 1:1 volumetric mixture of MDA-MB-231 cells in Matrigel, with an approximate number of cells of 1.5x10^6 per flank. The tumors were allowed to grow for around 3 weeks, or until they reached a volume of approximately 20 mm^3, as measured by the Vevo 770 system.

Two groups of mice were investigated: DDDs and empty nanodroplets. For each formulation used, one of the tumors was randomly selected to be subjected to activation, while the other served as internal control. This allowed us to discern between effects from the on-demand activation and passive accumulation/release of the DDDs.

The mice received a tail-vein injection of 100 μL (with a concentration of 250 μg/mL paclitaxel, and 70 μg/mL doxorubicin, at a 5% v/v PFP concentration, corresponding to a 5x dilution from as-prepared DDDs). Following the tail vein injections of the nanodroplets, the mice were subjected to a series of ultrasound pulses (515 kHz, 5.7 MPa peak focal pressure, 10 cycles) spaced at 20 s, for a total duration of 10 min (Fig. 2A). The transducer was acoustically coupled to the mouse with a custom-molded polyacrylamide cone (Fig. 2B). 3D-printed crosshairs were attached to the custom-built transducer holder to enable visual alignment of the ultrasound focus and the tumor. The activation sequence was started immediately after the tail vein injection. Mice were anesthetized by isofluorane (VetOne), at a 2% concentration in oxygen, with a flow rate of 1.5 L/h for all the procedures and measurements.

The tumor size was measured periodically using the Vevo 770 high-frequency ultrasound imaging system, together with the weight of the mice, and animals were sacrificed after 21 days after the nanodroplet

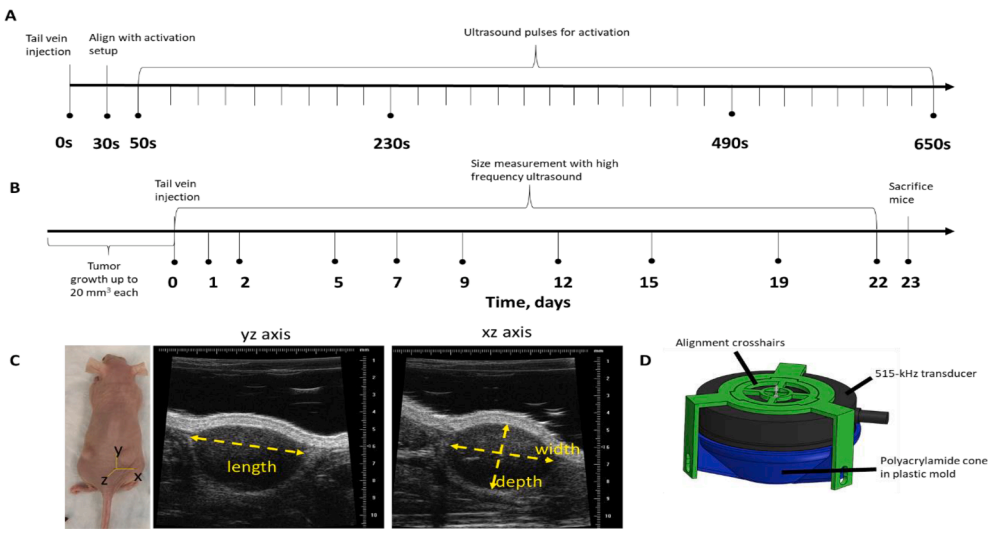

Fig. 2. A. Schematic of activation and ultrasound acquisition regimen showing the total duration and the spacing of ultrasound pulses; **B.** Timeline of tumor size measurements and spacing for the duration of the study, beginning once both tumors on a mouse reach at least 20 mm^3 volume; **C.** A mouse in the prone position showing the directions of measuring with the ultrasound transducer: along the yz axis for the length of the tumor, and an orthogonal frame of the tumor, on the xz axis, used to measure the depth and width of the tumor, respectively. **D** The *in-vivo* experiments used an annular 515-kHz ultrasound transducer. The hollow center aperture allowed for visual alignment of the ultrasound focus using 3D-printed crosshairs.

injection (Fig. 2B), or when meeting the euthanasia criteria (i.e., loss of more than 10% body weight or tumor burden larger than 300 mm^3). A 40-MHz single-element ultrasound transducer mounted on a motorized stage was used for tumor size measurements, raster scanning the tumor across the width (xz axis) across 10 mm, with a step of 0.1 mm. A cross-section of the tumor was also acquired. The tumor volume was computed by:

$$v = \frac{4\pi}{3}\left(\frac{averagelength}{2}\right) \bullet \left(\frac{width}{2}\right) \bullet \left(\frac{depth}{2}\right) \quad (3)$$

where the average length is obtained by an average of the length across three slices, and the width and depth are obtained from the orthogonal slice (Fig. 2C).

3. Results and discussion

3.1. Synthesis and size characterization of nanodroplets

The average hydrodynamic diameters of the nanodroplets as measured by dynamic light scattering were 332 ± 14 nm with a polydispersity index of 0.21 ± 0.01 immediately following the synthesis and washing steps (Fig. 3B). This size is within the range of what is considered acceptable for tumor extravasation, with previous studies determining the endothelial gap size around 400–600 nm [30,31]. Apart from size, physico-chemical properties like the surface charge influence the fate of nanoparticles during circulation, as well as through their extravasation and distribution through the tumor tissue [32]. In the case of our nanodroplets, zeta potential measurements indicated slightly negatively charged nanodroplets, with a z-average of −24 ± 1 mV (Fig. 3C). Moderately negatively charged particles, have been shown to have better stability in circulation due to reduced interaction with plasma proteins compared to positively-charged particles [33,34], as well as better transport through the extracellular matrix within the tumor issue after extravasation [35].

3.2. Nanodroplets drug encapsulation and release

Encapsulation efficiencies were measured to be approximately 74.6% for paclitaxel and 60.7% for doxorubicin (Fig. 4A), corresponding to a loading of 416 ± 113 μg/mL of paclitaxel, and 108 ± 21 μg/mL for doxorubicin (Fig. 4B). This translates into a loading of 38 mg paclitaxel/g nanodroplets and 10 mg doxorubicin/g nanodroplets. While this study kept the parameters constant, as to get the same ratio between loaded paclitaxel and loaded doxorubicin, the relatively simple synthesis method allows for this ratio to be modified. This allows for versatility in the effects of the nanodroplets, as different types of cells have been shown to have different optimal ratios for maximum treatment efficacy [27].

The activation of nanodroplets in dispersion, using 1.1-MHz ultrasound pulses of 10 cycles each, was undertaken, showing an increase in the recorded paclitaxel in the supernatant (34% increase relative to control), as well as doxorubicin (76% increase compared to control), indicating that a portion of the nanodroplets were vaporized and release their payload. Due to the focused nature of the sonication, we expect a relatively small proportion of nanodroplets to be activated. Moreover, the difference of released drug percentages between the two drugs was previously investigated in our work focusing on in vitro characterization of dual-drug loaded nanodroplets [36], concluding that the charge of the particles plays an important role in the separation procedure involved in the measurement of DOX, which does not impact the paclitaxel measurement in the same way.

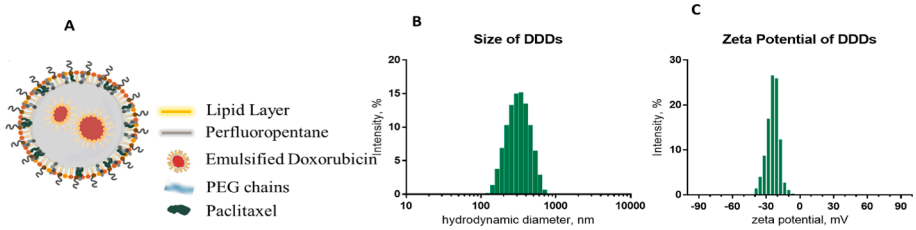

Fig. 3. A. Schematic of dual-drug loaded nanodroplets with a lipid shell and a perfluoropentane core containing paclitaxel (shell) and emulsified doxorubicin (core); **B.** Intensity-weighed DDDs size distribution; **C.** Intensity-weighed DDDs zeta potential distribution. The size and zeta potential distributions represent the average across 3 samples.

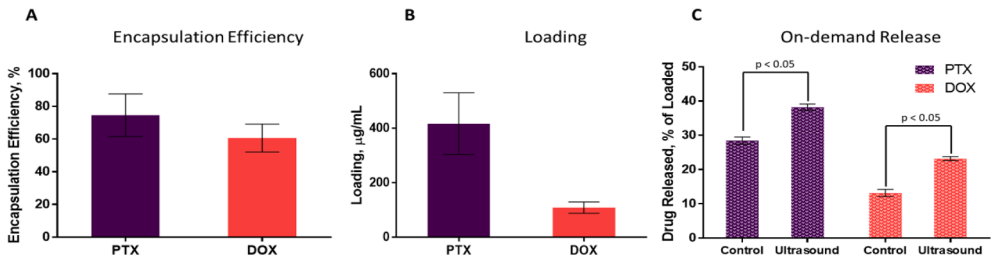

Fig. 4. A. Encapsulation efficiency of DDDs for both paclitaxel and doxorubicin; **B.** Loading (μg/mL) of both paclitaxel and doxorubicin of DDDs; **C.** Percentage of drug released from DDDs after activation with 10 pulses of 1.1-MHz ultrasound, 10 cycles each, at 9.6 MPa focal pressure. Each measurement represents the mean and standard deviation of 3 samples per experimental group.

3.3. Nanodroplets cytotoxicity

Dual drug-loaded droplets were tested for their cytotoxicity on MDA-MB-231 cells using an MTT assay. MDA-MB-231 cells are a well-established triple negative breast cancer cell line, and both paclitaxel and doxorubicin are used in therapeutic regimens for this type of disease in combination with one another [37,38] or other chemotherapeutics [39–41]. We compared the effect of incubating cells with drug-free nanodroplets against that of DDDs (Fig. 5). Drug-free nanodroplets, either activated or non-activated, showed no significant cytotoxic effect compared to the control cell group. There was also no significant difference between the activated and non-activated empty droplets, showing the mechanical effects of the expansion experiences during activation did not considerably affect cell viability. In contrast, activated DDDs showed lower cell viability than inactivated DDDs ($p = 0.032$). Non-activated DDDs did show some instability, recording a statistically significant cytotoxicity when compared to the cells group ($p = 0.0002$). We hypothesize this is due to the prolonged incubation time, which allowed for the nanodroplets to interact with the lipid membrane of cells, potentially releasing some of the lipophilic paclitaxel through lipid transfer [42]. Moreover, compared to cells that were subjected to a combination of free doxorubicin and paclitaxel in the same concentrations as the DDDs, the activated DDDs showed significantly greater cytotoxicity ($p = 0.0047$).

3.4. In-vivo biodistribution

Nu/Nu female mice with two hind-flank tumors were administered fluorescent DiR-loaded nanodroplets through a tail vein injection, followed by activation with high-intensity focused ultrasound of one of the tumors (515 kHz, pulses with 10 cycles each, spaced at 20 s between pulses for a total of 10 min).

The fluorescence signal in mice was followed prior to the injection, as well as post injection and activation at 30 min, 60 min, and 120 min. The mice included in this study showed relatively localized activated spots after activation, due to the small focus of the ultrasound transducer, and a slight increase in the fluorescence signal compared to the non-activated tumor within the span of the 120 min (Fig. 6A). After excising and imaging both tumors on all mice, a statistically significant difference in the signal between the two was observed (Fig. 6A-B, $p = 0.0027$ with a paired *t*-test). Although the results show higher accumulation of the DiR dye in the activated tumor, it does not necessarily indicate that extravasation occurred. A future study using cardiac perfusion to remove excess dye/nanodroplets in the blood stream could help confirm the delivery of payload into the interstitial space.

In a small additional study of two mice, the major organs were also excised and imaged for fluorescence signal (Fig. S1 A, Table S1). This showed the distribution of the signal in the major organs, with a majority of fluorescence being in the liver and spleen. The tumors contained 1.5–3.5% of the total fluorescence signal at this timepoint. These results are strong when compared to other nanoparticle platforms, which demonstrate tumor accumulation of 1% on average [38].

3.5. In-vivo dual-drug nanodroplets evaluation

To understand the effect that the nanodroplets have in the animal

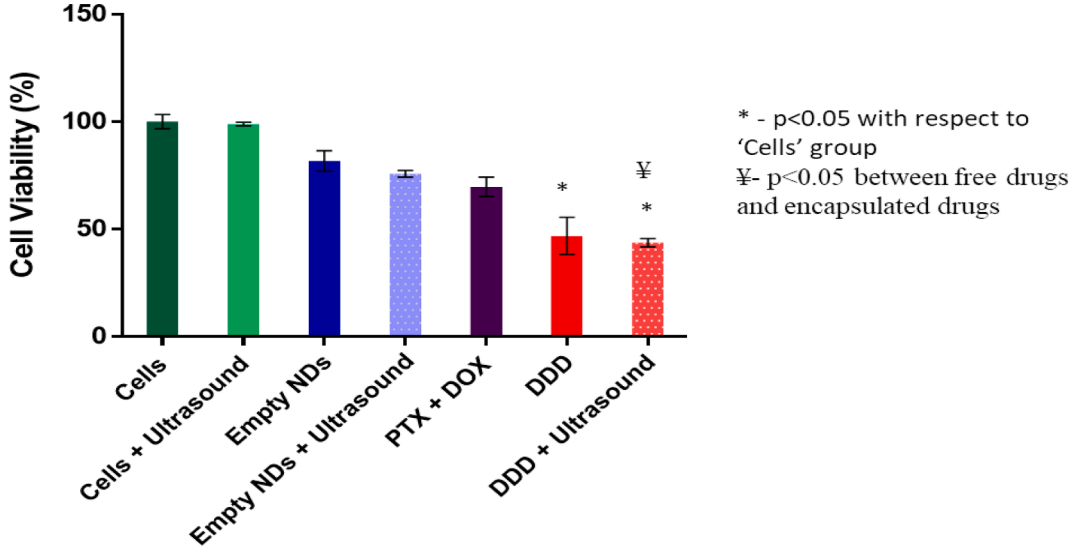

Fig. 5. Comparison of the cytotoxic effect on MDA-MB-231 cells of ultrasound alone, empty nanodroplets (non-activated and activated with ultrasound), free paclitaxel and doxorubicin, and dual-drug nanodroplets (non-activated and activated with ultrasound). For the activated samples, 10 pulses of 1.1-MHz ultrasound, 10 cycles each, at 9.6 MPa focal pressure was applied. N = 3 for each experimental group.

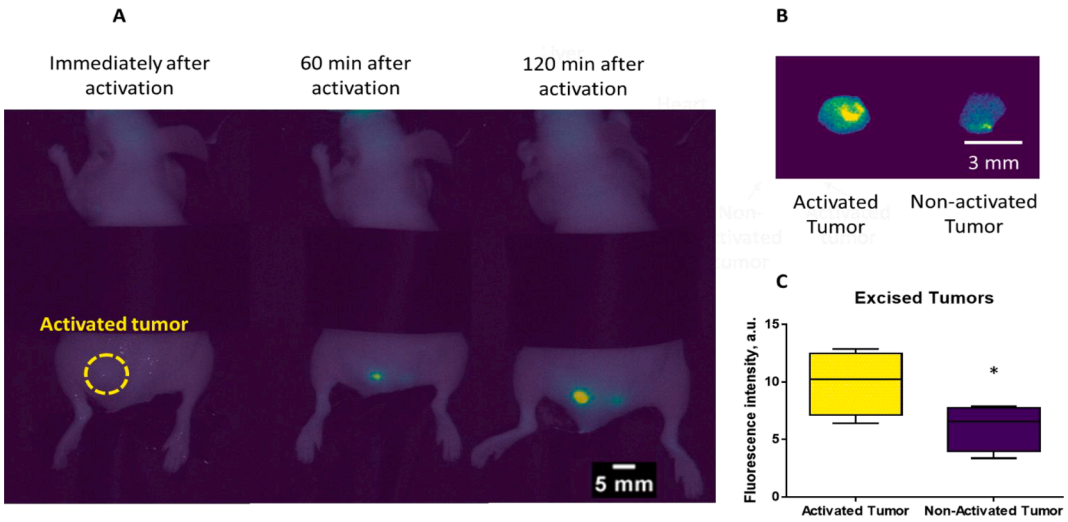

Fig. 6. A. Overlay of fluorescence and white images of a mouse with two hind leg tumors that received a DiR nanodroplets tail vein injection imaged: immediately after activation of one of the tumors, 60 min after activation, and 120 min after activation, respectively; **B.** Example of activated and non-activated tumor excised from the same mouse; **C.** Boxplot graph of the fluorescence intensity in excised tumors that were activated vs non-activated counterparts (N = 3). * indicates a p = 0.0027.

model, a study was setup to compare mice receiving DDDs with mice receiving non-loaded, or empty nanodroplets. The model was the same as described in the fluorescent droplets study, with two hind tumors one of which was activated with focused ultrasound, and the other used as internal control. The tumor size was followed periodically after the injection and activation for both groups, and the weight of mice was also recorded at several timepoints to ensure that the treatment was not negatively affecting the mice. In the case of dual-drug loaded nanodroplets, a one-dose regimen was used. Empty nanodroplets were administered at the same PFP concentration.

Over the duration of the study, the dual-drug nanodroplets receiving mice showed a delay in the tumor growth rate compared to the non-sonicated counterparts (Fig. 7A-B), as shown by a paired *t*-test (p = 0.0002). Performing individual paired t-tests between the data for the 5 mice at each timepoint showed a statistically significant difference between the tumor volumes at days 2 (p = 0.034), 5 (p = 0.009), 7 (p = 0.0002). This is not unexpected, as the effect of drugs is expected to occur in the first few days after administration and taper off, with clinical regimens usually dosing paclitaxel and doxorubicin over an interval from 3 h to 24 h and repeating the treatment every two or three weeks, depending on the type, location and aggressiveness of the tumors in question [43,44]. However, with nanoparticles' efficiency of accumulating in tumors being generally low, concerns about off-target toxicity can impair the repeated administration. Histology samples taken from a mouse receiving an intravenous injection of DDDs at the same dose as the mice in the tumor growth rate study showed no deleterious effects on normal tissue in liver, spleen, kidneys, and heart. At the same time, the tumors presented with regions where cell death was underway, with the activated tumor also including a hemorrhage, potentially from the mechanical effects of the activation (Fig. S.2).

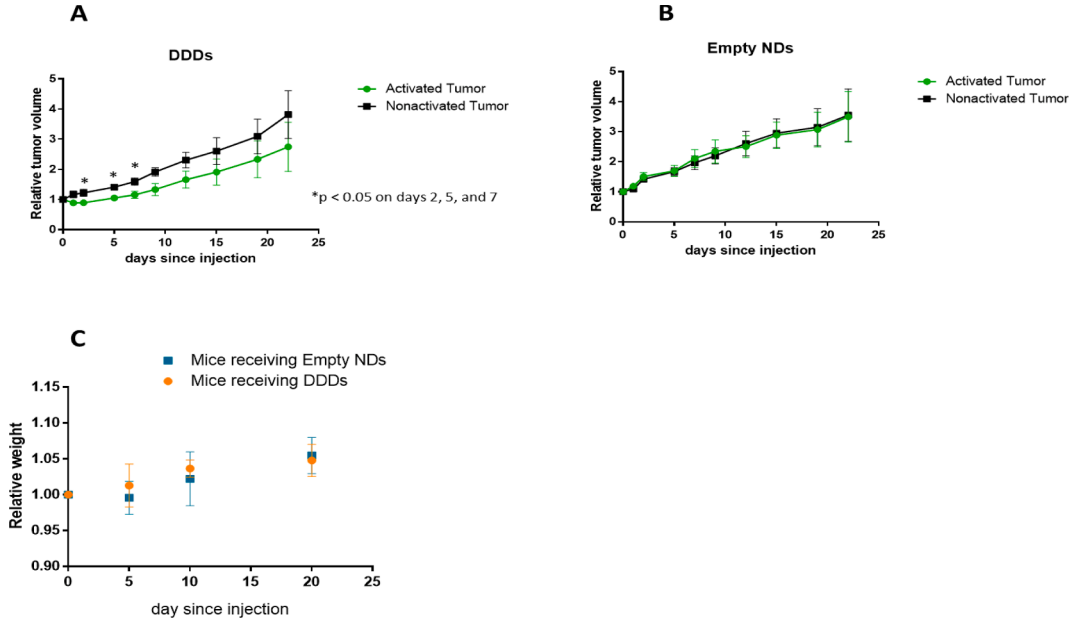

Fig. 7. A. Aggregate tumor growth rate for activated tumors compared to non-activated counterparts on mice that received a DDDs injection (N = 5); **B.** Aggregate tumor growth rate for activated tumors c2ompared to non-activated counterparts on mice that received an empty nanodroplets injection (N = 5); **C.** Weight evolution of mice receiving either DDDs or empty nanodroplets injections on day 0, expressed as relative ratio with respect to the mice's weight on day 0.

Therefore, we expect that a repeated dosage, of nanodroplet-encapsulated drugs could be most beneficial, in not only slowing the rate of growth, but actively reducing the size.

Meanwhile, mice injected with empty nanodroplets showed no difference in their tumor growth rates (Fig. 7B). This indicates that the cytotoxic effect noticed in the case of dual-drug loaded droplets is due to the chemotherapeutics rather than the mechanical effects of the activation on the tumor tissue. This is an important aspect, particularly in the case of multiple-dose regimens, as damaging the vasculature of the tumor in an irreversible way could lead to a decrease in nanodroplets that reach the tumor in subsequent administrations. All 5 mice in the study showed the lack of a statistically significant difference, compared to the DDDs-receiving group, where some variability in the intensity of the response was recorded (Fig. S.3).

The evolution of the weight of mice in both groups was similar, with no obvious difference being noticeable between the groups (Fig. 7C), which correlates with the histology data that did not show damage in the major organs.

4. Conclusions

In this work, we report the construction and characterization of phase-changing nanodroplets loaded with both paclitaxel and doxorubicin for ultrasound-triggered drug-releasing capabilities. The two chemotherapeutics are concurrently loaded into a core–shell nanodroplet structure, with a PFP core and a biocompatible lipid shell. The activation results in expulsion of the loaded drugs in the specific region of interest.

We characterized the cytotoxicity of the DDDs, noting an enhancement in the effect of triggered nanodroplets compared to free drug formulations. Similarly, *in-vivo* studies showed that ultrasound-activated DDDs slowed tumor growth compared to tumors that did not receive activation, and empty nanodroplets recorded no benefit from activation in terms of tumor growth.

The DDDs combined two synergistic drugs with different pharmacokinetic profiles. By using the same nanocarrier, the delivery dynamics were matched. The platform is versatile and could be modified to carry other combinations of drugs. Some combinations, however, can be antagonistic, making it preferable to deliver the drugs at different times [45]. In this case, it may be a better strategy to use two separate formulations of nanodroplets delivered independently.

However, work remains to be done towards increasing the amount of nanodroplets that extravasate into the tumor. The ultrasound intensity was selected to be relatively high in order to ensure DDD vaporization, but the number of cycles and number of pulses was kept low to prevent thermal or mechanical damage. Extended sonication duration could possibly help promote drug delivery beyond the vasculature via stable and inertial cavitation. In addition, the ultrasound was applied immediately after the injection of the DDDs to activate them while circulating through the tumor vasculature. It may be beneficial to wait for some accumulation prior to activation. The center frequency of the ultrasound transducer also plays an important role in nanodroplet vaporization and mechanical effects on the tissue [46]. Although we used a different transducer to facilitate the *in-vivo* studies, a full characterization of DDD activation and payload delivery should be performed using multiple frequencies.

Finally, it will be important to incorporate ultrasound imaging of the drug release process. We have previously demonstrated that similar ultrasound stimuli produce gaseous bubbles from similar nanodroplets that can visualized with ultrasound imaging [47]. Thus, imaging could be used to estimate the delivered dose. In addition, imaging could provide more insight into whether acoustic droplet vaporization or some other destructive mechanism is responsible for the drug release.

Overall, our work proposes a nanocarrier design with on-demand drug-release for enhanced efficacy combination therapy that can be activated non-invasively using ultrasound, allowing for more control over localization of the cytotoxic effect of chemotherapeutics.

Declaration of Competing Interest

The authors declare that they have no known competing financial interests or personal relationships that could have appeared to influence the work reported in this paper.

Data availability

Data will be made available on request.

Acknowledgements

This work was supported by the PhD Innovation Program at the Thayer School of Engineering, Hanover, NH.

Appendix A. Supplementary material

Supplementary data to this article can be found online at https://doi.org/10.1016/j.ultras.2023.107056.

References

[1] D. Hanahan, R.A. Weinberg, Hallmarks of cancer: the next generation, Cell 144 (2011) 646–674.
[2] R.B. Mokhtari, et al., Combination therapy in combating cancer, Oncotarget 8 (2017) 38022.
[3] X. Xu, W. Ho, X. Zhang, N. Bertrand, O. Farokhzad, Cancer nanomedicine: from targeted delivery to combination therapy, Trends Mol. Med. 21 (2015) 223–232.
[4] F. Kratz, A. Warnecke, Finding the optimal balance: challenges of improving conventional cancer chemotherapy using suitable combinations with nano-sized drug delivery systems, J. Control. Release 164 (2012) 221–235.
[5] L.D. Mayer, A.S. Janoff, Optimizing combination chemotherapy by controlling drug ratios, Mol. Interv. 7 (2007) 216.
[6] J. Fang, W. Islam, H. Maeda, Exploiting the dynamics of the EPR effect and strategies to improve the therapeutic effects of nanomedicines by using EPR effect enhancers, Adv. Drug Deliv. Rev. 157 (2020) 142–160.
[7] F. Danhier, To exploit the tumor microenvironment: Since the EPR effect fails in the clinic, what is the future of nanomedicine? J. Control. Release 244 (2016) 108–121.
[8] G. Lanza, et al., Theragnostics for tumor and plaque angiogenesis with perfluorocarbon nanoemulsions, Angiogenesis 13 (2010) 189–202.
[9] N. Rapoport, Drug-loaded perfluorocarbon nanodroplets for ultrasound-mediated drug delivery, Therapeutic ultrasound 221–241 (2016).
[10] J. Kim, et al., Perfluorocarbon nanodroplets versus microbubbles in cavitation-enhanced sonothrombolysis of retracted clots, J. Acoust. Soc. Am. 146 (2019) 2775.
[11] N. Rapoport, R. Gupta, Y.-S. Kim, B.E. O'Neill, Polymeric micelles and nanoemulsions as tumor-targeted drug carriers: insight through intravital imaging, J. Control. Release 206 (2015) 153–160.
[12] N. Rapoport, Phase-shift, stimuli-responsive perfluorocarbon nanodroplets for drug delivery to cancer, Wiley Interdiscip. Rev. Nanomed. Nanobiotechnol. 4 (2012) 492–510.
[13] M.L. Fabiilli, J.A. Lee, O.D. Kripfgans, P.L. Carson, J.B. Fowlkes, Delivery of water-soluble drugs using acoustically triggered perfluorocarbon double emulsions, Pharm. Res. 27 (2010) 2753–2765.
[14] O. Couture, et al., Ultrasound internal tattooing, Med. Phys. 38 (2011) 1116–1123.
[15] Z. Yuan, A. Demith, R. Stoffel, Z. Zhang, Y.C. Park, Light-activated doxorubicin-encapsulated perfluorocarbon nanodroplets for on-demand drug delivery in an in vitro angiogenesis model: comparison between perfluoropentane and perfluorohexane, Colloids Surf. B Biointerfaces 184 (2019), 110484.
[16] N. Rapoport, et al., Ultrasound-mediated tumor imaging and nanotherapy using drug loaded, block copolymer stabilized perfluorocarbon nanoemulsions, J. Control. Release 153 (2011) 4–15.
[17] N. Al Rifai, et al., Ultrasound-triggered delivery of paclitaxel encapsulated in an emulsion at low acoustic pressures, J. Mater. Chem. B 8 (2020) 1640–1648.
[18] D. Qin, et al., In situ observation of single cell response to acoustic droplet vaporization: membrane deformation, permeabilization, and blebbing, Ultrason. Sonochem. 47 (2018) 141–150.
[19] K.A. Hallam, S.Y. Emelianov, Toward optimization of blood brain barrier opening induced by laser-activated perfluorocarbon nanodroplets, Biomed. Opt. Express 10 (2019) 3139, https://doi.org/10.1364/BOE.10.003139.
[20] M. Aryal, C.D. Arvanitis, P.M. Alexander, N. McDannold, Ultrasound-mediated blood–brain barrier disruption for targeted drug delivery in the central nervous system, Adv. Drug Deliv. Rev. 72 (2014) 94–109.
[21] Y.-J. Ho, C.-K. Yeh, Theranostic performance of acoustic nanodroplet vaporization-generated bubbles in tumor intertissue, Theranostics 7 (2017) 1477.
[22] S.M. Fix, A. Novell, Y. Yun, P.A. Dayton, C.B. Arena, An evaluation of the sonoporation potential of low-boiling point phase-change ultrasound contrast agents in vitro, J. Ther. Ultrasound 5 (2017) 1–11.

[23] S. Snipstad, S. Hanstad, A. Bjørkøy, Ý. Mørch, C. de Lange Davies, Sonoporation using nanoparticle-loaded microbubbles increases cellular uptake of nanoparticles compared to co-incubation of nanoparticles and microbubbles, Pharmaceutics 13 (2021) 640.
[24] J. Tu, A.C. Yu, Ultrasound-mediated drug delivery: sonoporation mechanisms, biophysics, and critical factors, BME Front. 2022 (2022).
[25] L. Biganzoli, et al., Doxorubicin-paclitaxel: a safe regimen in terms of cardiac toxicity in metastatic breast carcinoma patients. Results from a European Organization for Research and Treatment of Cancer multicenter trial, Cancer: Interdisciplinary Int. J. Am. Cancer Soc. 97 (2003) 40–45.
[26] M. Airoldi, et al., Paclitaxel and pegylated liposomal doxorubicin in recurrent head and neck cancer: clinical and unexpected pharmacokinetic interactions, Anticancer Res. 28 (2008) 2519–2527.
[27] H. Baabur-Cohen, et al., In vivo comparative study of distinct polymeric architectures bearing a combination of paclitaxel and doxorubicin at a synergistic ratio, J. Control. Release 257 (2017) 118–131.
[28] S. Jandhyala, A. Van Namen, C.-P. Spatarelu, G.P. Luke, EGFR-targeted perfluorohexane nanodroplets for molecular ultrasound imaging, Nanomaterials 12 (2022) 2251.
[29] T. Jordan, J.M. Newcomb, M.B. Hoppa, G.P. Luke, Focused ultrasound stimulation of an ex-vivo Aplysia abdominal ganglion preparation, J. Neurosci. Methods 372 (2022), 109536.
[30] J. Di, et al., Size, shape, charge and "stealthy" surface: carrier properties affect the drug circulation time in vivo, Asian J. Pharm. Sci. 16 (2021) 444–458.
[31] F. Yuan, et al., Vascular permeability in a human tumor xenograft: molecular size dependence and cutoff size, Cancer Res. 55 (1995) 3752–3756.
[32] J.A. Mills, F. Liu, T.R. Jarrett, N.L. Fletcher, K.J. Thurecht, Nanoparticle based medicines: approaches for evading and manipulating the mononuclear phagocyte system and potential for clinical translation, Biomater. Sci. 10 (2022) 3029–3053.
[33] E. Beltrán-Gracia, A. López-Camacho, I. Higuera-Ciapara, J.B. Velázquez-Fernández, A.A. Vallejo-Cardona, Nanomedicine review: Clinical developments in liposomal applications, Cancer Nanotechnol. 10 (2019) 1–40.
[34] H. Ren, et al., Role of liposome size, surface charge, and PEGylation on rheumatoid arthritis targeting therapy, ACS Appl. Mater. Interfaces 11 (2019) 20304–20315.
[35] O. Lieleg, R.M. Baumgärtel, A.R. Bausch, Selective filtering of particles by the extracellular matrix: an electrostatic bandpass, Biophys. J. 97 (2009) 1569–1577.
[36] C.-P. Spatarelu, A. Van Namen, G.P. Luke, Optically activatable double-drug-loaded perfluorocarbon nanodroplets for on-demand image-guided drug delivery, ACS Appl. Nano Mater. 4 (2021) 8026–8038.
[37] M. Teshome, K.K. Hunt, Neoadjuvant therapy in the treatment of breast cancer, Surg. Oncol. Clin. 23 (2014) 505–523.
[38] R. Bartsch, E. Bergen, A. Galid, Current concepts and future directions in neoadjuvant chemotherapy of breast cancer, memo-Magazine Eur. Med. Oncol. 11 (2018) 199–203.
[39] A. Marra, G. Viale, G. Curigliano, Recent advances in triple negative breast cancer: the immunotherapy era, BMC Med. 17 (2019) 1–9.
[40] L. Biganzoli, et al., Management of elderly patients with breast cancer: updated recommendations of the International Society of Geriatric Oncology (SIOG) and European Society of Breast Cancer Specialists (EUSOMA), Lancet Oncol. 13 (2012) e148–e160.
[41] Y.-C. Cheung, et al., Monitoring the size and response of locally advanced breast cancers to neoadjuvant chemotherapy (weekly paclitaxel and epirubicin) with serial enhanced MRI, Breast Cancer Res. Treat. 78 (2003) 51–58.
[42] M. Aron, O. Vince, M. Gray, C. Mannaris, E. Stride, Investigating the role of lipid transfer in microbubble-mediated drug delivery, Langmuir 35 (2019) 13205–13215.
[43] M. Untch, et al., Nab-paclitaxel versus solvent-based paclitaxel in neoadjuvant chemotherapy for early breast cancer (GeparSepto—GBG 69): a randomised, phase 3 trial, Lancet Oncol. 17 (2016) 345–356.
[44] L. Gianni, et al., Phase III trial evaluating the addition of paclitaxel to doxorubicin followed by cyclophosphamide, methotrexate, and fluorouracil, as adjuvant or primary systemic therapy: European Cooperative Trial in Operable Breast Cancer, J. Clin. Oncol. 27 (2009) 2474–2481.
[45] N. Yin, et al., Synergistic and antagonistic drug combinations depend on network topology, PLoS One 9 (2014) e93960.
[46] B. Glickstein, et al., Nanodroplet-mediated low-energy mechanical ultrasound surgery, Ultrasound Med. Biol. 48 (2022) 1229–1239.
[47] A. Van Namen, S. Jandhyala, T. Jordan, G.P. Luke, Repeated acoustic vaporization of perfluorohexane nanodroplets for contrast-enhanced ultrasound imaging, IEEE Trans. Ultrason. Ferroelectr. Freq. Control 68 (2021) 3497–3506, https://doi.org/10.1109/TUFFC.2021.3093828.